

**Electronic supplementary materials** *Mendeleev Commun.*, 2023, **33**, 209–211

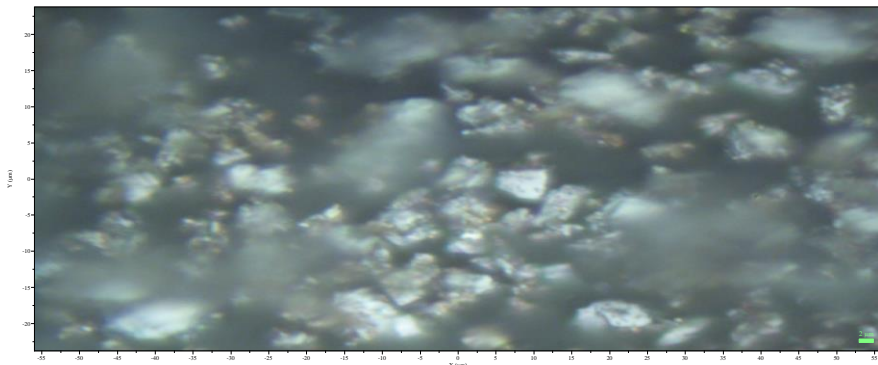
## Laser induced metastable phases in microcrystalline silicon

**Sergey S. Bukalov and Rinat R. Aysin**

### Experimental details

$\text{Si}_{\text{Met}}$  plates used for microelectronics crushed in ball mill VEB Narva Vibrator DDR-GM 9458 for 2–10 min. Weighed portion  $\text{Si}_{\text{Met}}$  was  $\sim 100$  mg in standard stainless steel mortar with two 10 mm WC balls.

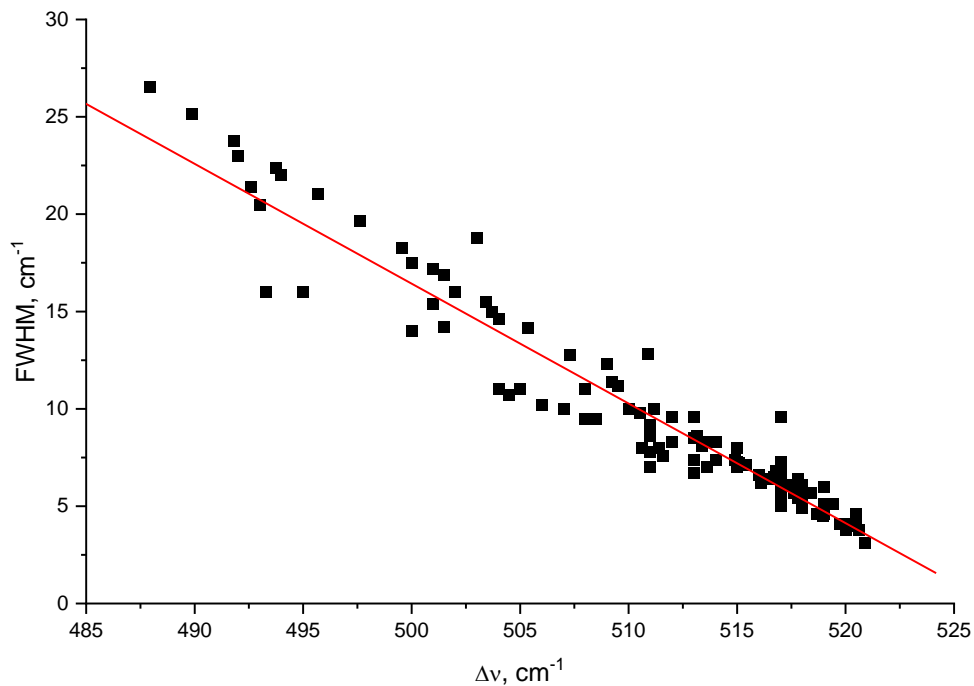
Raman spectra in 80–3500  $\text{cm}^{-1}$  region were registered with using a Horiba JobinYvon Labram 300 spectrometer equipped Olympus BX2 microscope (Olympus M-Plan 50x and 100x lens), cooled CCD detector and excitation 632.8 nm He-Ne laser with power on sample up to 3 mW. The  $\sim 500$  spectra were registered with laser beam focusing up to 1  $\mu\text{m}$  circle. The heating of  $\mu\text{-Si}$  particles from 25 to 300  $^{\circ}\text{C}$  was performed using a Linkam heating stage. Conversion of power to radiation density is impractical due to non-plane surface of  $\mu\text{-Si}$  particles.



**Figure S1.** The photographs for Si microparticles.

**Table S1.** The parameters for the TO mode at different power

Power, mW	Power increasing		Power decreasing	
	$\Delta\nu, \text{cm}^{-1}$	FWHM, $\text{cm}^{-1}$	$\Delta\nu, \text{cm}^{-1}$	FWHM, $\text{cm}^{-1}$
0.03	520.4	4.4	520.5	4.4
0.3	519.3	5.1	519.1	5.0
0.75	517.5	5.7	517.5	5.6
1.5	512.2	8.4	512.3	8.2
3	501.7	17.2	501.7	17.2

**Figure S2.** The position and FWHM correlation of the TO mode for microcrystalline Si<sub>Met</sub> ( $\mu$ -Si).

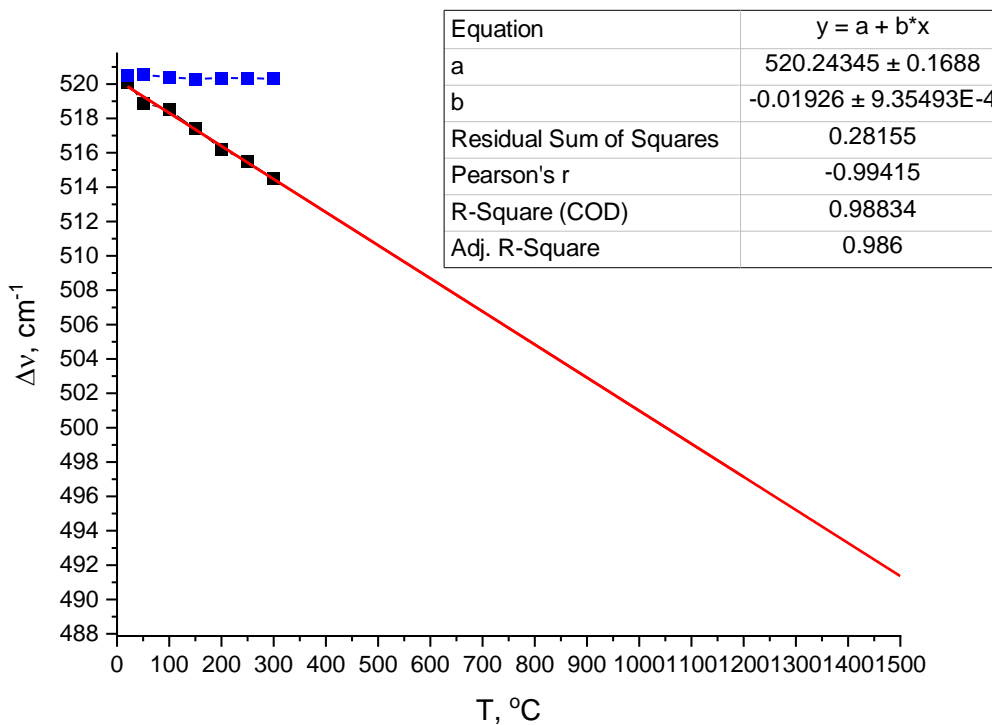


**Figure S3.** Temperature dependence and approximation of the TO mode position for microcrystalline Si<sub>Met</sub> (red) in comparison to that for Si plate (blue).

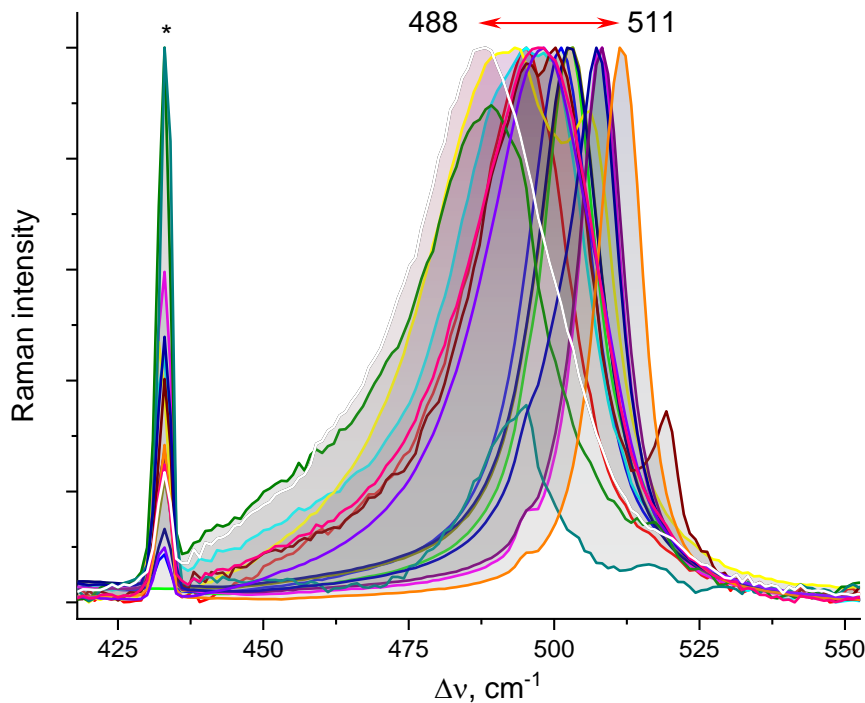


**Figure S4.** The TO mode position at 3 mW laser excitation power for different size Si particles (2 – 35  $\mu$ m). \* – the plasma line.

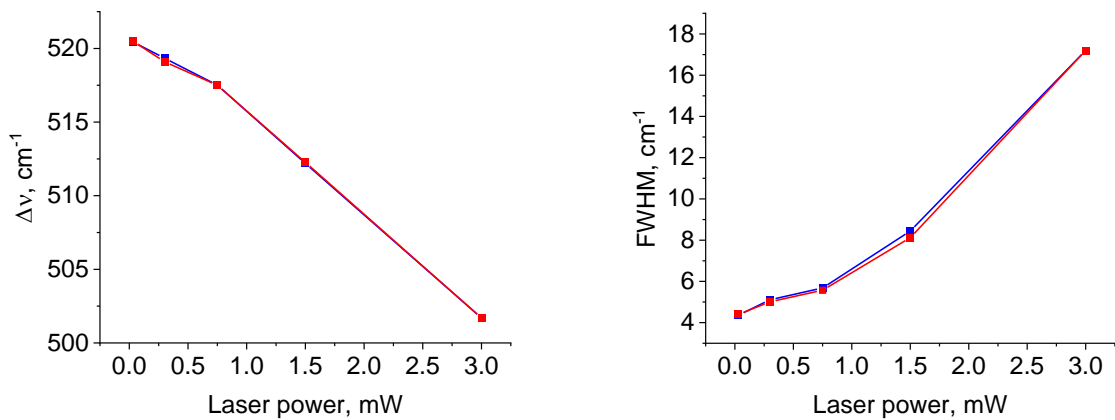


**Figure S5.** The dependence of the TO mode position (left) and its FWHM (right) during increasing (red) and decreasing (blue) laser power.

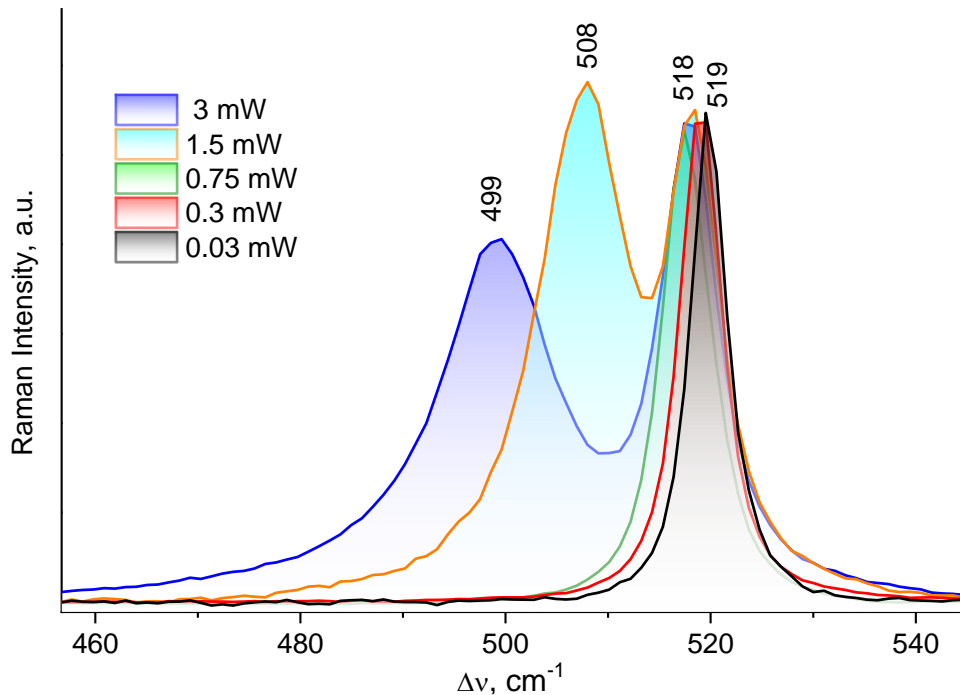


**Figure S6.** The splitting of TO mode corresponding to metastable phases.

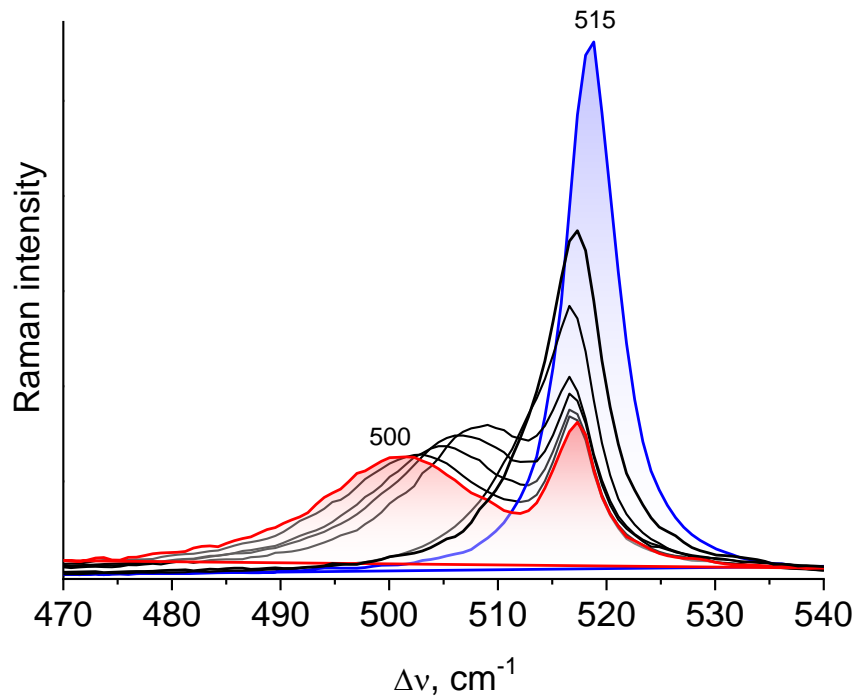


**Figure S7.** The series of Raman spectra for the fast annealing process (during 6 hours) of metastable phase in  $\mu$ -Si. Red line is initial spectrum, blue line is final.

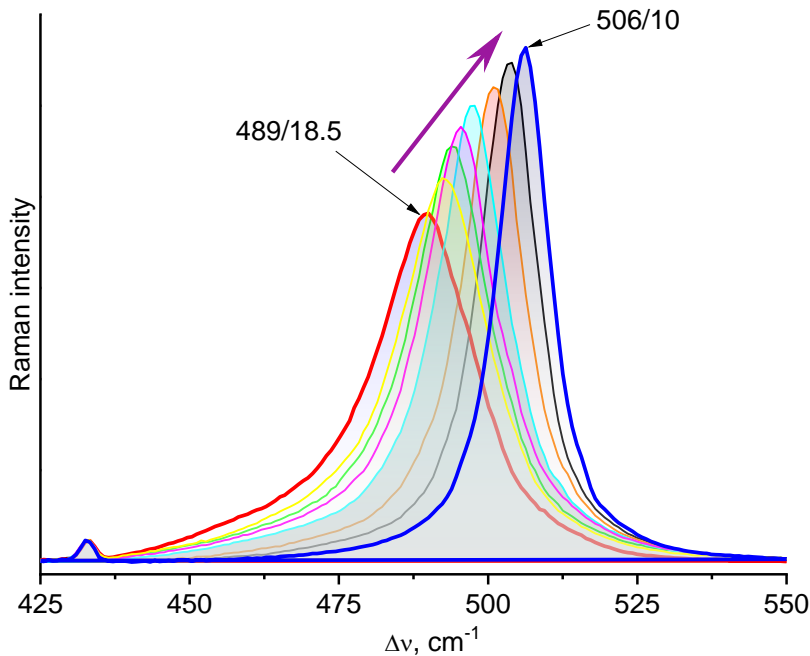


**Figure S8.** The series of Raman spectra for the annealing process of metastable phase in  $\mu$ -Si during 2 days. Red line is initial spectrum, blue is final.

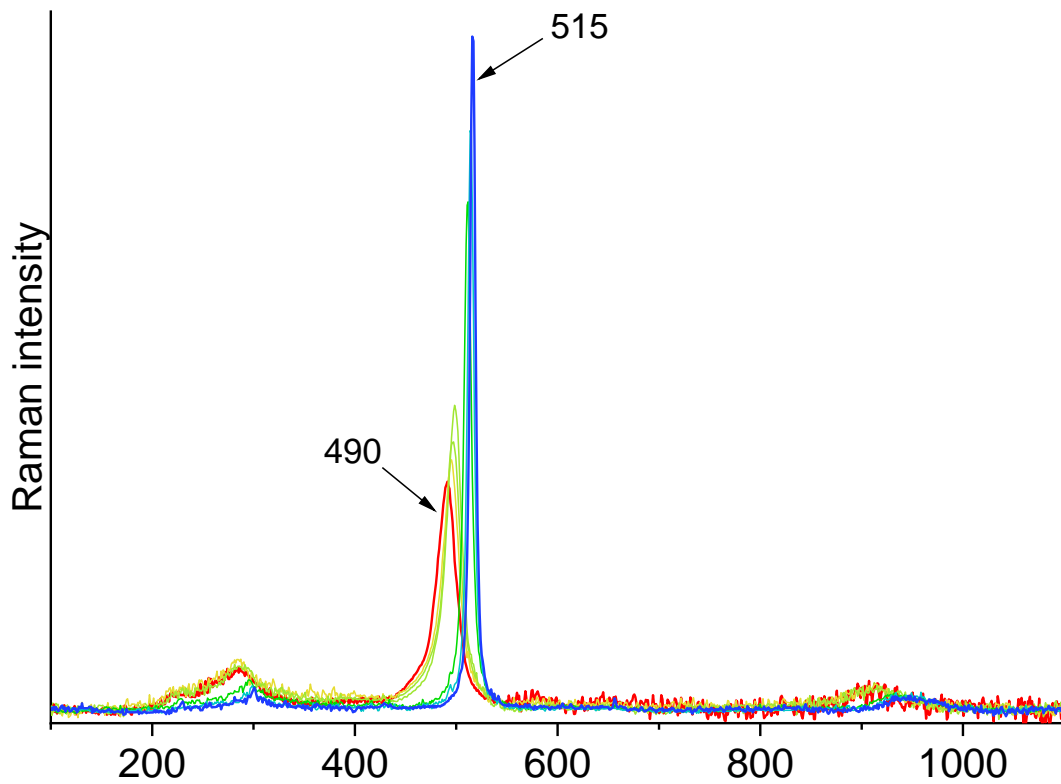


**Figure S9.** The series of Raman spectra (full range) for the annealing process of metastable phase in  $\mu$ -Si during 4 days. Red line is initial spectrum, blue is final. Baseline is corrected.

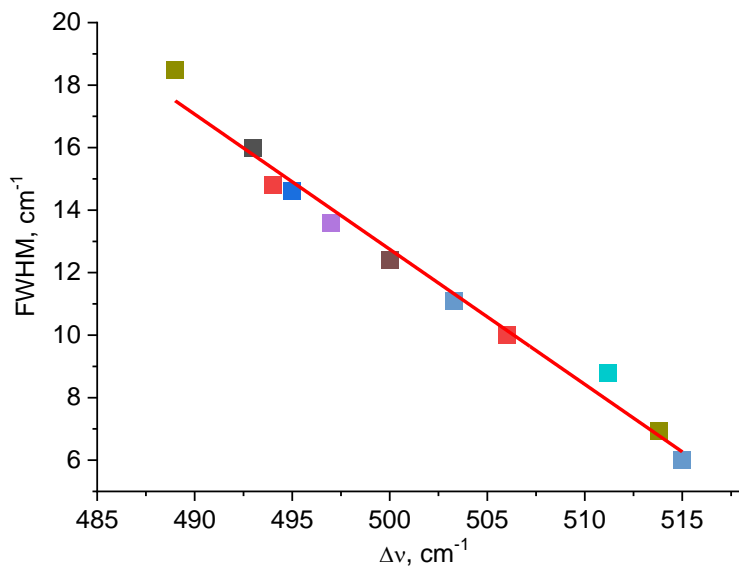


**Figure S10.** The correlation of the position and FWHM values obtained from Fig. S9.